World Applied Sciences Journal 18 (12): 1813-1824, 2012
ISSN 1818-4952

DOI: 10.5829/idosi.wasj.2012.18.12.2486

Comparison between Homotopy Perturbation and Modified Adomian Decomposition Methods in Simulating the Effect of Van der Waals Attraction in Nano Structures Instability

[1]Gholamhosein Amirbostaghi, [1]Sahar Khatibi, [2]Mariam K Hafshejani and [3]Armin Arad

[1]Zanjan Branch, Islamic Azad University, Zanjan, Iran
[2]Shahrekord University of Medical Sciences, Shahrekord, Iran
[3]North Khorasan University of Medical Sciences, Bojnurd, Iran

Abstract: In recent years, the instability of nano scale structures has become of great interest for scientists. In this work the ability of Homotopy perturbation and modified Adomian decomposition methods for modeling the effect of Van der Waals attraction in the nonlinear instability of cantilever and doubly-supported Carbon Nano Tubes (CNT) based bio sensor and nano bio sensor is comparatively investigated. The critical value system deflection at the onset of the instability is computed as the basic parameter for sensor applications. It is found that using Homotopy perturbation method (HPM) in solving nano structures problems can lead to physically incorrect results. The values of the instability parameters computed by HPM series converge to the values which originally differ from those obtained by numerical methods. Even more, in the case of doubly-supported CNT or nano sensor, the conventional series diverge from numerical solution as the number of series terms increases. These shortcomings are not observed for modified Adomian series.

Key words: Bio sensor . nonlinear differential equation . homotopy perturbation . modified adomian decomposition . instability

INTRODUCTION

Recently nano-cantilever based biosensors become one of the most components in evaluating live systems. These systems transform bio molecular reactions at the nano scale into mechanical work at multiple nano-, meso- and macroscopic length scales [1-5]. Cantilever sensors offer the unique ability to convert bio molecular reactions occurring on one side of the cantilever into mesoscopic bending moment for bio sensing and smart nano-robotic applications. The low-cost sensors not only show fast response, high sensitivity and suitable for parallelization intoarrays, but also provide common platforms for label-free analysis such as DNA hybridization, antigen-antibody binding and drug discovery [6-11]. One of the main advantages of the cantilever sensors is the ability to detect interacting compounds without the need of introducing an optically detectable label on the binding entities. In the recent years, very exciting and significant advances in biochemical detection have been made using cantilever sensors. Direct, label-free detection of DNA and proteins have been demonstrated (Fig. 1) using silicon cantilevers [12]. By applying nano-scale continuum models the governing equation of free standing CNT based sensor and cantilever bio sensor can be derived as [13-19]:

$$y^{(IV)} + f_n x^{-n} = 0 \qquad (n = 3,4,5) \tag{1}$$

In recent decades, various mathematical methods, such as Adomian decomposition [20, 21], variational iteration [22, 23], homotopy perturbation [24, 25], etc. have been proposed for solving nonlinear problems. The decomposition method proposed by Adomian has been widely used to solve stochastic systems [26-30] and engineering problems [17, 29-30]. due to the convenience of the computations. Several investigators made attempt to improve Adomian decomposition [31, 32]. Rach [28] proposed a systematic formula for computing the

Corresponding Author: Gholamhosein Amirbostaghi, Zanjan Branch, Islamic Azad University, Zanjan, Iran

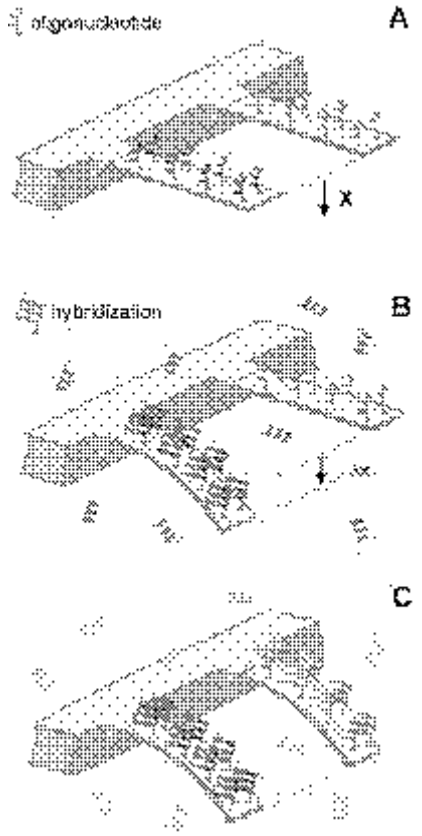

Fig. 1: Detection of label-free DNA hybridization using nano mechanical cantilevers [3]

Adomian's polynomials. Further modification of the polynomials was also provided by Gabet [32]. A powerful modification of the Adomian decomposition method was proposed by Wazwaz [33]. This modification highly accelerates the convergence of the decomposition polynomials and it is applied for solving higher order boundary value problems [34-36]. homotopy perturbation was first proposed by He [24] and was used to solve nonlinear engineering and other problems [13-16, 37, 38] The major drawback of traditional perturbation technique is the over dependence on the existence of very small parameter [39]. This condition restricts the applications of perturbation method in solving strongly nonlinear problems which do not contain the so-called small parameter. However HPM method does not depend on a small parameter. It has been shown that HPM is powerful and convenient technique that can effectively solve a large class of highly nonlinear problems with comp onents converging rapidly to accurate solutions [13-15, 39-42].

Herein, the limitations/advantages of Homotopy Perturbation and modified Adomian decomposition (MAD) methods in solving constitutive equation of CNT and NEMS (equation (1)) are investigated. In addition, numerical solution is obtained using MAPLE commercial software and presented solutions are compared with the numerical results. The precision and convergence speed of both methods are compared.

GOVERNING EQUATION

Freestanding nano sensor: Figure 2 depicts schematic cantilever and doubly-supported nao sensor suspended over a fixed electrode with small gap between them. Based on continuum mechanics, the governing equation of a freestanding nano switch with rectangular section with widths of b and thickness of t by considering the Van der Waals attraction can be derived as [30]:

$$E_{eff} I \frac{d^4U}{dX^4} = \frac{Aw}{6p(g-U)^3} \quad (2a)$$

$$U(0)=\frac{dU(0)}{dX}=\frac{d^2U(L)}{dX^2}=\frac{d^3U(L)}{dX^3}=0 \text{ for cantilever beam} \quad (2b)$$

$$U(0)=\frac{dU}{dX}(0)=U(L)=\frac{dU}{dX}(L)=0 \text{ for doubly-supported beam} \quad (2c)$$

where A is the Hamaker constant, X is the position along the NEMS measured from the clamped end(s) and U is the deflection of NEMS. The length of NEMS is L and the initial gap between NEMS and the ground is g. Equations (2a-d) can be made dimensionless using the following substitutions:

$$x = X/L \quad (3a)$$

$$u=\frac{U}{g} \quad (3b)$$

$$f_3=\frac{AwL^4}{6\pi g^4 E_{eff} I} \quad (3c)$$

These transformations yield,

$$\frac{d^4u}{dx^4}=\frac{f_3}{(1-u(x))^3} \quad (4a)$$

$$u(0)=u'(0)=0 \text{ (BC. For Cantilever and Doubly-supported nano switch)} \quad (4b)$$

$$u''(1)=u'''(1)=0 \text{ (BC. For Cantilever nano switch)} \quad (4c)$$

$$u(1)=u'(1)=0 \text{ (BC. For Doubly-supported nano switch)} \quad (4d)$$

Note that at the onset of the buckling instability, the maximum deflection of the NEMs increases abruptly. In mathematical view, the slope of u-f_3 curve reaches infinity when instability occurs, i.e. $du/df_3(x=1)\to 8$ and $du/df_3(x=0.5)\to 8$ for cantilever and doubly-supported nano switch, respectively. As a convenient approach, the values of critical van der Waals force, f_3^* and the corresponding switch critical deflection can be acquired via plotting u(x=1) vs. f_3 for cantilever and u(x=0.5) vs. f_3 for doubly-supported switch. In order to apply HPM and MAD methods for simulating the deflection and the instability of NEMS, the substitution y=1-u is used to rewrite equation (4) into the following form:

$$\frac{d^4y}{dx}=-\frac{f_3}{y(x)^3} \quad (5a)$$

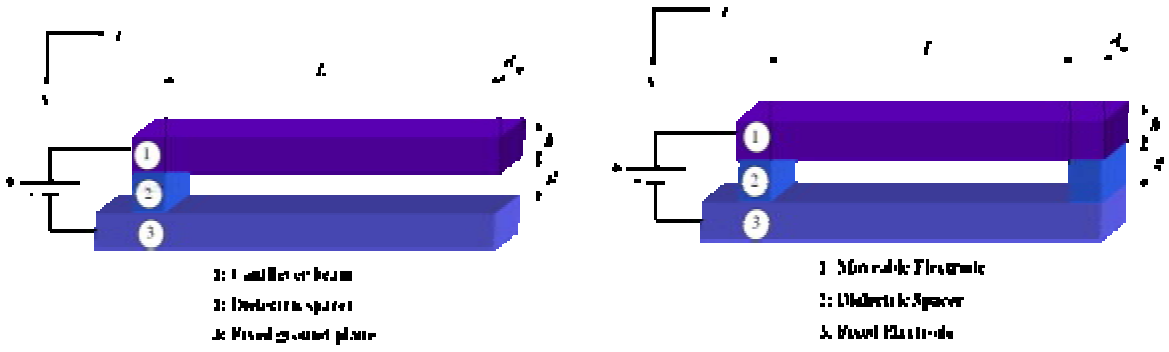

(a) (b)

Fig. 2: Schematic representation of the nano-beam: (a) Cantilever (b) Doubly-supported

$$y(0) = 1,\ y'(0) = 0 \tag{5b}$$

$$y''(1) = 0,\ y'''(1) = 0 \text{ (For Cantilever nano switch)} \tag{5c}$$

$$y(1) = 1,\ y'(1) = 0 \text{ (For Doubly-supported nano switch)} \tag{5d}$$

CNT based sensor: Figure 3 depicts schematic cantilever and doubly-supported CNT based sensors suspended over graphite with small gap between them. With the decrease in dimensions from micro to nano-scale, CNT deflects to the substrate due to the van der Waals interaction between CNT and graphite. Especially, when the separation is sufficiently small, the nanotube becomes unstable and buckles onto the graphite layers. Based on continuum mechanics, the governing equation of a freestanding single-walled CNT over graphite surface can be derived as [16]:

$$E_{eff} I \frac{d^4 U}{dX^4} = \begin{cases} \dfrac{C_6 \sigma^2 \pi^2 R}{d(D-U)^4} & \text{For large number of graphene layers} \\ \dfrac{4C_6 \sigma^2 \pi^2 NR}{(D-U+Nd/2)^5} & \text{For small number of graphene layers} \end{cases} \tag{6a}$$

$$U(0) = \frac{dU}{dX}(0) = 0 \tag{6b}$$

$$\frac{d^2 U}{dX^2}(L) = \frac{d^3 U}{dX^3}(L) = 0 \text{ (For Cantilever CNT)} \tag{6c}$$

$$U(L) = \frac{dU}{dX}(L) = 0 \text{ (For Doubly-supported CNT)} \tag{6d}$$

where X is the position along the CNT measured from the clamped end(s) and U is the deflection of CNT. The length of CNT is L and the initial gap between CNT and the ground is D. In above relation, E_{eff}, I, σ and C_6 are the CNT Young's modulus, cross-sectional moment of inertia, graphene surface density and attractive constant, respectively. The constants d and N are the graphite interlayer distance and number of layers, respectively. Equations (6a-d) can be made dimensionless using the following substitutions:

$$x = X/L \tag{7a}$$

$$u = \begin{cases} \dfrac{U}{D} & \text{For large number of layers} \quad (n = 4) \\ \dfrac{U}{D + Nd/2} & \text{For small number of layers} \quad (n = 5) \end{cases} \tag{7b}$$

$$f_n = \begin{cases} \dfrac{C_6 \sigma^2 \pi^2 R L^4}{dE_{eff} I D^5} & \text{For large number of layers} \quad (n = 4) \\ \dfrac{4C_6 \sigma^2 \pi^2 NRL^4}{E_{eff} I (D + Nd/2)^6} & \text{For small number of layers} \quad (n = 5) \end{cases} \tag{7c}$$

These transformations yield,

$$\frac{d^4 u}{dx^4} = \frac{f_n}{(1-u(x))^n} \tag{8a}$$

$$u(0) = u'(0) = 0 \text{ (BC. For Cantilever and Doubly-supported CNT)} \tag{8b}$$

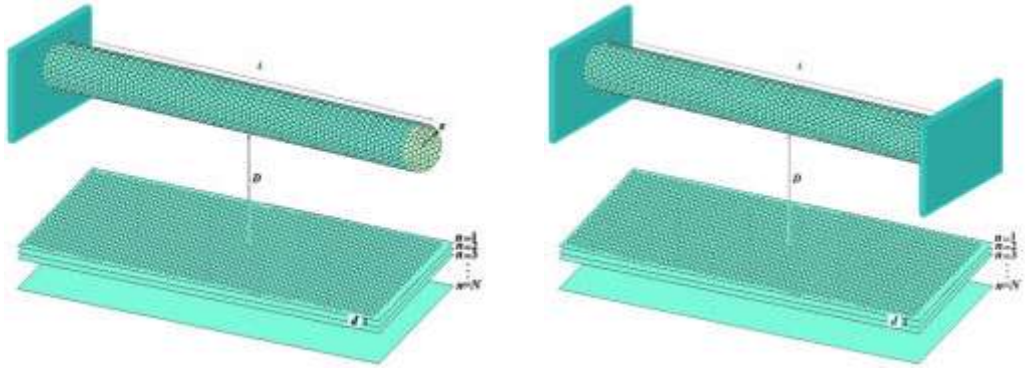

(a) (b)

Fig. 3: A CNT over a graphite ground plane (a) Cantilever CNT (b) doubly-supported CNT

$$u''(1) = u'''(1) = 0 \text{ (BC. For Cantilever CNT)} \tag{8c}$$

$$u(1) = u'(1) = 0 \text{ (BC. For Doubly-supported CNT)} \tag{8d}$$

Note that at the onset of the buckling instability, the maximum deflection of the CNT increases abruptly. In mathematical view, the slope of u-f_n curve reaches infinity when instability occurs, i.e. $dw/df_n(z=1)\rightarrow 8$ and $du/df_n(x=0.5)\rightarrow 8$ for cantilever and doubly-supported CNT, respectively. As a convenient approach, the values of critical van der Waals force, f_n^* and the corresponding CNT critical deflection can be acquired via plotting u(x=1) vs. f_n for cantilever and u(x=0.5) vs. f_n for doubly-supported CNT. In order to apply decomposition methods for simulating the deflection and the instability of CNT, the substitution y=1-u is used to rewrite equation (14) into the following form:

$$\frac{d^4y}{dx} = -\frac{f_n}{y(x)^n} \quad (n = 3,4) \tag{9a}$$

$$y(0) = 1,\ y'(0) = 0 \tag{9b}$$

$$y''(1) = 0,\ y'''(1) = 0 \text{ (For Cantilever CNT)} \tag{9c}$$

$$y(1) = 1,\ y'(1) = 0 \text{ (For Doubly-supported CNT)} \tag{9d}$$

SOLUTION METHODS

Homotopy perturbation solution: To illustrate the basic ideas of homotopy-perturbation method for solving non-linear differential equations, the following equation is considered [24]:

$$A(u) - f(s) = 0, s \in \Omega \tag{10}$$

with boundary conditions

$$B\left(u, \frac{\partial u}{\partial n}\right) = 0, s \in \Gamma \tag{11}$$

where A is a general differential operator, B is a boundary operator, f(s) is a known analytical function and ? is the boundary of the domain ? . The operator A can be divided into linear, L and nonlinear, N, parts. Therefore, equation (10) can be rewritten as follows:

$$L(u) + N(u) - f(s) = 0, s \in \Omega \tag{12}$$

The structure of homotopy perturbation method is constructed as follows:

$$H(y,p) = (1-p)\left[L(y) - L(u_0)\right] + p\left[A(y) - f(s)\right] = 0 \tag{13}$$

where

$$y(s,p): \Omega \times [0,1] \to R \tag{14}$$

In equation (13), $p \in [0, 1]$ is an embedding parameter and u_0 is the first approximation that satisfies the boundary condition. It is assumed that the solution of equation (12) can be written as a power series in terms of p, as following:

$$y = \sum_{k=0}^{\infty} p^k y_k = y_0 + py_1 + p^2 y_2 + p^3 y_3 + \cdots \tag{15}$$

and the best approximation for the solution is

$$u = \lim_{p \to 1} y = \lim_{p \to 1} \sum_{k=0}^{\infty} p^k y_k = y_0 + y_1 + y_2 + y_3 + \cdots \tag{16}$$

The above convergence is discussed in [24].

Using the transformation dy/dx=w(x), dw/dx=v(x), dv/dx=z(x), we can rewrite the boundary value problem (equation (1)) as a system of differential equations:

$$\frac{dy}{dx} = w(x) \tag{17a}$$

$$\frac{dw}{dx} = v(x) \tag{17b}$$

$$\frac{dv}{dx} = z(x) \tag{17c}$$

$$\frac{dz}{dx} = -\frac{f_n}{y(x)^n} \tag{17d}$$

with y(0)=1, w(0)=0, v(0)=A, z(0)=B, which A and B are second and third derivative of y with respect to x at x=0, respectively.

Integrating equation 17(a-d), we get the following system of integral equations:

$$y(x) = 1 + \int_0^x w(t)dt \tag{18a}$$

$$w(x) = 0 + \int_0^x v(t)dt \tag{18b}$$

$$v(x) = A + \int_0^x z(t)dt \tag{18c}$$

$$z(x) = B - \int_0^x \left(f_n\, y(x)^{-n}\right)dt \tag{18d}$$

Substituting equation (15) in equation 18(a-d), we have

$$\sum_{k=0}^{\infty} p^k y_k = 1 + \int_0^x \left(\sum_{k=0}^{\infty} p^k w_k \right) dt \tag{19a}$$

$$\sum_{k=0}^{\infty} p^k w_k = 0 + \int_0^x \left(\sum_{k=0}^{\infty} p^k v_k \right) dt \tag{19b}$$

$$\sum_{k=0}^{\infty} p^k v_k = A + \int_0^x \left(\sum_{k=0}^{\infty} p^k z_k \right) dt \tag{19c}$$

$$\sum_{k=0}^{\infty} p^k z_k = B - \int_0^x \left(f_n \sum_{k=0}^{\infty} p^k \varphi_{k,n} \right) dt \tag{19d}$$

The functions $\varphi_{k,n}$ approximating the nonlinear term y_k^{-n} are determined in Taylor series [25],

$$\phi_{k,n} = \frac{1}{k!} \frac{d^k}{dp^k} \left[\left(\sum_{i=0}^{\infty} p^i y_i \right)^{-n} \right]_{p=0} \tag{20}$$

The expansion of above relation is given in appendix A. With comparing the coefficient of similar powers of p, see Appendix B, the solution of equation (1) can be summarizing to:

$$\begin{aligned} u(x) = {} & -Ax - \frac{Bx^2}{2!} - \frac{Cx^3}{3!} + \frac{(\alpha+\beta+\gamma\beta)}{1+\delta}\frac{x^4}{4!} - \frac{(4\alpha+2\beta+\gamma\beta)}{1+\delta}\frac{Ax^5}{5!} + \left[\frac{2(10\alpha+3\beta+\gamma\beta)A^2}{1+\delta} - \frac{(4\alpha+2\beta+\gamma\beta)B}{1+\delta}\right]\frac{x^6}{6!} \\ & + \left[-\frac{(20\alpha+4\beta+\gamma\beta)6A^3}{1+\delta} + \frac{(10\alpha+3\beta+\gamma\beta)6B}{1+\delta} - \frac{(4\alpha+2\beta+\gamma\beta)C}{1+\delta}\right]\frac{x^7}{7!} + \left[\frac{(35\alpha+5\beta+\gamma\beta)24A^4}{1+\delta} - \frac{(20\alpha+4\beta+\gamma\beta)36A^2B}{1+\delta}\right. \\ & \left. + \frac{(5\alpha+3\beta+\beta)6B^2}{1+\delta} + \frac{(10\alpha+3\beta+\gamma\beta)8AC}{1+\delta} + \frac{(4\alpha+2\beta+\gamma\beta)(\alpha+\beta+\gamma\beta)}{1+\delta}\right]\frac{x^8}{8!} + ... \end{aligned} \tag{21}$$

The unknown coefficients A and B can obtain from boundary conditions u"(1)=0 and u'"(1)=0.

Modified Adomian (MAD) series solution: In order to solve equation (1) by MAD analytical method, consider the following fourth-order boundary-value problem:

$$y^{(4)}(x) = f(x,y), \qquad 0 \le x \le L_b \tag{22a}$$

$$y(0) = \alpha_0, \qquad y'(0) = \alpha_1 \tag{22b}$$

Equation (22-a) can be represented as:

$$L^{(4)}\left[y(x)\right] = f(x,y) \tag{23}$$

where $L^{(n)}$ and its corresponding inverse operator $L^{(-n)}$ are the n-fold differential and integral operators respectively, which are define as

$$L^{(n)} = \frac{d^{(n)}}{dx^{(n)}} \tag{24-a}$$

$$L^{-(n)} = \underbrace{\int_0^x \ldots \int_0^x (.)\, dx \ldots dx}_{n} \tag{24-b}$$

Employing the MAD method [27, 28], the dependent variable in equation (22) can be written as:

$$y(x)=\sum_{n=0}^{\infty} y_n(x) \tag{25}$$

According to [39] and using the relations (22) and (25), the following recursive equations can be provided:

$$\begin{aligned} &y_0(x)=\alpha_0 \\ &y_1(x)=\alpha_1 x+\frac{1}{2}C_1x^2+\frac{1}{3!}C_2x^3+L^{-(4)}[A_0] \\ &y_{n+1}(x)=L^{-(4)}[A_k] \end{aligned} \tag{26}$$

In the above relations the coefficient A_k is determined from the nonlinear part of the function f(x,y) (N[f]) via the MAD polynomials:

$$N[f]=\sum_{n=0}^{\infty} A_n \tag{27}$$

Refer to [26] it can further be presented as the following convenient equations

$$A_n=\sum_{v=1}^{n} C(v,n)h_v(f_0) \tag{28}$$

where

$$C(v,n)=\sum_{p_i}\prod_{i=1}^{v}\frac{1}{k!}f_{p_i}^{k_i} \tag{29}$$

and k_i is the number of repetition in the f_{pi}, the values of p_i are selected from the following range by combination without repetition

$$\sum_{i=1}^{v} k_i p_i=n;\quad n>0,\ 0\le i\le n,\ 1\le p_i\le n-v+1 \tag{30}$$

In equation (28), $h_v(f_0)$ is calculated by differentiating the nonlinear terms of f, v times with respect to g at $\lambda=0$ and can be represented as follows:

$$h_v(f_0)=\frac{d^v}{dg^v}[f(\lambda)]_{\lambda=0} \tag{31}$$

Hence, it is convenient to obtain the Adomian polynomials as:

$$\begin{aligned} &A_0=h_0(f_0) \\ &A_1=C(1,1)h_1(g_0)=f_1h_1(f_0) \\ &A_2=C(1,2)h_1(f_0)+C(2,2)h_2(f_0)=f_2h_1(f_0)+\frac{1}{2!}f_1^2h_2(f_0) \\ &A_3=C(1,3)h_1(f_0)+C(2,3)h_2(f_0)+C(3,3)h_3(f_0) \\ &\quad=f_3h_1(f_0)+f_1f_2h_2(f_0)+\frac{1}{3!}f_1^3h_3(f_0) \\ &\cdots\cdots \end{aligned} \tag{32}$$

Now by using relations (32), the series terms y_n are obtained from recursive relations (26) as the followings:

$$
\begin{aligned}
&y_0 = 1\\
&y_1 = \frac{1}{2!}C_1x^2 + \frac{1}{3!}C_2x^3 - \frac{f_n}{4!}x^4\\
&y_2 = nf_n\left(\frac{1}{6!}C_1x^6 + \frac{1}{7!}C_2x^7 - \frac{1}{8!}f_nx^8\right)\\
&y_3 = -3n(n+1)f_n\frac{C_1^2}{8!}x^8 - 10n(n+1)\frac{C_1C_2}{9!}f_nx^9 + \frac{n^2C_1 + n(n+1)(15C_1 - 10C_2^2)}{10!}f_n^2x^{10}\\
&+\frac{(n^2 + 35n(n+1))C_2}{11!}f_n^2x^{11} - \frac{n^2f_n^2 + 35n(n+1)f_n^3}{12!}x^{12}
\end{aligned}
\tag{33}
$$

Therefore, the solution of equation (1) can be summarized to:

$$
\begin{aligned}
u(x) = &-C_1\frac{x^2}{2!} - C_2\frac{x^3}{3!} + f_n\frac{x^4}{4!} - C_1nf_n\frac{x^6}{6!} - C_2nf_n\frac{x^7}{7!} + (3n(n+1)C_1^2 + nf_n)f_n\frac{x^8}{8!} + 10n(n+1)C_1C_2f_n\frac{x^9}{9!}\\
&-\left(n^2C_1 + n(n+1)(15C_1 - 10C_2^2)\right)f_n^2\frac{x^{10}}{10!} - (n^2 + 35n(n+1))f_n^2C_2\frac{x^{11}}{11!} + \left(n^2f_n^2 + 35n(n+1)f_n^3\right)\frac{x^{12}}{12!} + \ldots
\end{aligned}
\tag{34}
$$

The unknown coefficients C_1 and C_2 can obtain from boundary conditions u"(1)=0 and u"'(1)=0.

CASE STUDIES AND COMPARISON OF THE METHODS

To compare HPM and MAD methods, typical cantilever and doubly-supported CNT and nano switch are modeled using both mentioned decomposition methods and the results are compared with numerical solution.

Cantilever case: Figure 4 shows the variation of tip deflection (u(x=1)) of typical cantilever CNT/NEMS (f_n=0.5) obtained by HPM and MAD methods using various series terms. As seen, the MAD series converges faster to the numerical solution in comparison with the HPM series.

When f_n exceeds the critical value, f_n^*, no solution exists for w and the buckling occurs. Table 1 shows the convergence of instability characteristics (f_n^*) for cantilever CNT/NEMS obtained by various series terms. This table reveals that HPM converges to an instability value which is different from the numerical one. However, this shortcoming is not observed in the case of the MAD series and the instability value obtained by MAD method converges to that of numerical solution.

Double-cantilever case: Figure 5 shows the variation of mid-point deflection for doubly-supported CNT/NEMS (f_n=5) as a function of series terms. This figure reveals that conventional decomposition can not be applied for

Table 1: Convergence check of critical values of f (f_n^*) for cantilever case. Despite HPM, the f_n^* values obtained by MAD series converge to those of numerical values

	Method	3 Terms	5 Terms	6 Terms	8 Terms	10 Terms	Numerical
f_2^*	HPM	Can't determine	Can't determine	4	1.521	1.412	1.680
	MAD	2.179	1.739	Can't determine			
f_3^*	HPM	Can't determine	Can't determine	2.667	1.060	1.008	1.204
	MAD	1.508	1.234	Can't determine			
f_4^*	HPM	Can't determine	Can't determine	2	0.8146	0.7853	0.9391
	MAD	1.1551	0.9577	Can't determine			
f_5^*	HPM	Can't determine	Can't determine	1.6	0.6616	0.6434	0.7695
	MAD	0.9360	0.7827	Can't determine			

Table 2: The critical van der Waals force (f_n^*) for doubly-supported case

	1 terms	2 terms	3 terms	4 terms	5 terms	6 terms	Numerical
f_2^*	Can't determine f_n^*	Can't determine f_n^*	93.000	Can't determine f_n^*	71.758	Can't determine f_n^*	70.063
f_3^*	Can't determine f_n^*	Can't determine f_n^*	64.000	Can't determine f_n^*	50.750	Can't determine f_n^*	50.094
f_4^*	Can't determine f_n^*	Can't determine f_n^*	49.1626	Can't determine f_n^*	39.3133	Can't determine f_n^*	38.9976
f_5^*	Can't determine f_n^*	Can't determine f_n^*	39.8103	Can't determine f_n^*	32.1010	Can't determine f_n^*	31.9301

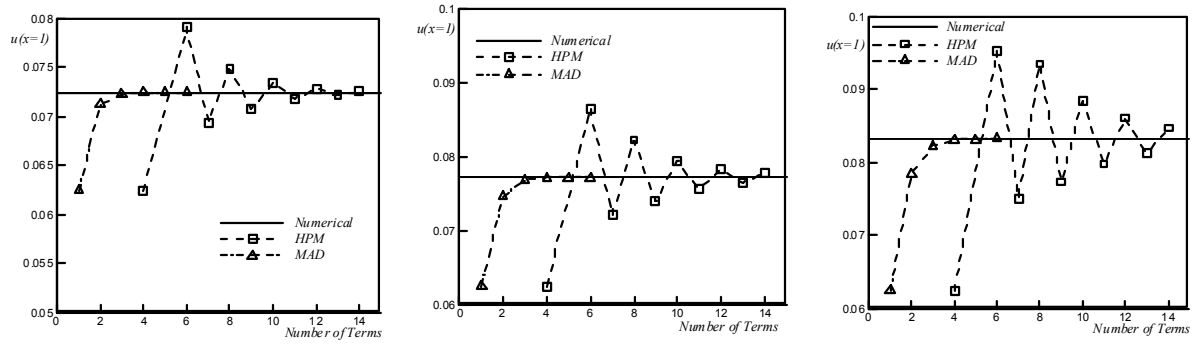

Fig. 4: Variation of tip deflection as a function of selected Adomian series terms for typical cantilever CNT/NEMS (f_n=0.5): (a) n=3, (b) n=4 (c) n=5

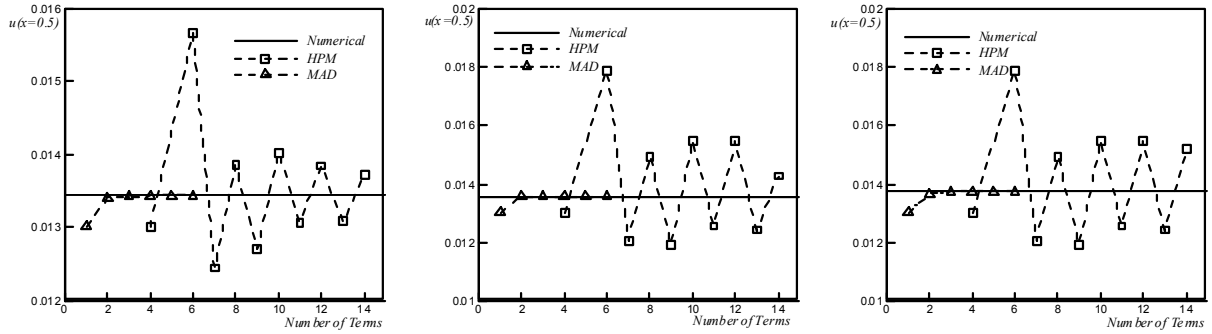

Fig. 5: Variation of tip deflection as a function of selected Adomian series terms for typical doubly-supported CNT/NESM (f_n=5): (a) n=3, (b) n=4 (c) n=5

modeling the CNT/NEMS deflection. As seen, while the MAD method rapidly converges to the numerical solution, HPM series diverges from it.

Furthermore, Table 2 shows the convergence of f_n^* for doubly-supported CNT/NEMS obtained by MAD using various series terms. As seen, f_n^* values obtained by MAD series converge to that of numerical value. In Table 1, only the f_n^* values obtained by MAD are presented since the HPM method is not able to model the double-supported CNT/NEMS. Note that while some series (Even term series) are able to approximate the CNT deflection (Fig. 5), they cannot determine the instability of the CNT. This limitation should be considered in simulations to avoid physically worthless results.

CONCLUSION

In this work, the Homotopy perturbation and modified Adomian decomposition methods are applied to simulate the mechanical behavior of cantilever and doubly-supported CNT and NEMS suspending over graphite surface or fixed electrode. The critical van der Waals force at the onset of the instability is computed and the results are compared with numerical solution.

Results reveal that Homotopy perturbation provides computational errors in simulating van der Waals force-induced deflection and instability of CNT/NEMS. The values of instability characteristics computed by HPM series converge to the values which differ from those obtained by numerical methods. Even more, in the doubly-supported case, the deflection value computed HPM series is very different from that of numerical method.

Interestingly, none of the mentioned shortcomings are observed for modified Adomian series. Compared to HPM method, the modified Adomian provides acceptable results, converges rapidly to numerical solution and can easily be utilized to simulate the instability of freestanding CNT and nano switch. Although some series can approximate the deflection (far from the instability point of the system), but they can not determine the instability of the nanotube and nano switches. This limitation should be considered in CNT and NEMS modeling to avoid physically meaningless results.

ACKNOWLEDGEMENT

This work is based on a research proposal founded by Islamic Azad University.

REFERENCES

1. Browne, W.R. and B.L. Feringa, 2006. Making molecular machines work. Nature Nanotechnology, 1: 25-35.
2. Feinberg, A.W., A.F. Sergey, S. Shevkoplyas, S. Sheehy, G.M. Whitesides and K.K. Parker, 2007. Muscular thin films for building actuators and powering devices. Science, 317: 1366-1370.
3. Bashir, B., 2004. BioMEMS: State-of-the-art in detection, opportunities and prospects. Advanced Drug Delivery Reviews, 56: 1565-1586
4. Ding, T.J., J.H. Lue, T.H. Yang, J.Yg. Chang and W.Y. Chen, 2012. Monitoring DNA Hybridization with a Simply Manufactured GMR Biosensor. Life Sci. J., 9 (2): 1015-1019.
5. Ding, T.J., J.H. Lue and T.H. Yang, 2012. Simple Embossing Process for Fabricating GMR Biosensor with Variable waveguide Thickness. Life Sci. J., 9 (2): 1020-1026.
6. Liu, F., Y. Zhang and Z. Ou-Yang, 2003. Flexoelectric origin of nanomechanic deflection in DNA-microcantilever system. Biosensors and Bioelectronics, 18: 655-660.
7. Alvarez, M., L.G. Carrascosa, M. Moreno, A. Calle, A.L. Zaballos, M. Lechuga, C. Martínez-A and J. Tamayo, 2004. Nanomechanics of the formation of DNA self-assembled monolayers and hybridization on microcantilevers. Langmuir, 20: 9663-9668.
8. Hansen, K.M. and T. Thundat, 2005. Microcantilever Biosensors. Methods, 37: 57-64.
9. Stachowiak, J.C., M. Yue, K. Castelino, A. Chakraborty and A. Majumdar, 2006. Chemomechanics of surface stresses induced by DNA hybridization. Langmuir, 22: 263-268.
10. Zhang, N.H. and J.Z. Chen, 2009. Mechanical properties of double-stranded DNA biolayers immobilized on microcantilever under axial compression. Journal of Biomechanics, 42: 1483-14837.
11. Azhir, E., R. Etefagh, N. Shahtahmasebi, M. Mohammadi, D. Amiri and R. Sarhaddi, 2012. Aspergillus niger biosensor based on tin oxide (SnO_2) nanostructures: nanopowder and thin film. Indian Journal of Science and Technology, 5 (7): 3010-3012.
12. Fritz, J., M.K. Baller, H.P. Lang, H. Rothuizen, P. Vettiger, E. Meyer, H. Guntherodt, C. Gerberand and J.K. Gimzewski, 2000. Translating Biomolecular Recognition into Nanomechanics. Science, 288: 316-318.
13. Abadyan, M., A. Novinzadeh and AS. Kazemi, 2010. Approximating the effect of Casimir force on the instability of electrostatic nanocantilevers. Physica Scripta, 81: 015801.
14. Abdi, J., A. Koochi, A.S. Kazemi and M. Abadyan, 2011. Modeling the Effects of Size Dependency and Dispersion Forces on the Pull-In Instability of Electrostatic Cantilever NEMS Using Modified Couple Stress Theory. Smart Materials and Structures, 20: 055011 (9pp).
15. Koochi, A., A. Noghrehabadi, M. Abadyan and E. Roohi, 2011. Investigation of the effect of van der Waals force on the instability of electrostatic Nano-actuators. International Journal of Modern Physics B, 25(29): 3965-3976.
16. Koochi, A., A.S. Kazemi and M. Abadyan, 2011. Simulating deflection and determining stable length of freestanding CNT probe/sensor in the vicinity of grapheme layers using a nano-scale continuum model. NANO, 6 (5): 419-429.
17. Koochi, A., A.S. Kazem, A. Noghrehabadi, A. Yekrangi and M. Abadyan, 2011. New approach to model the buckling of carbon nanotubes near graphite sheets. Materials and Design, 32 (5): 2949-2955.

18. Noghrehabadi, A., Y. Tadi Beni, A. Koochi, A.S. Kazemi, A. Yekrangi, M. Abadyan and M. Noghrehabadi, 2011. Closed-form Approximations of the Pull-in Parameters and Stress Field of Electrostatic Cantilever Nano-actuators Considering van der Waals Attraction. Procedia Engineering, 10: 3758-3764.
19. Abdi, J., Y. Tadi Beni, A. Noghrehabadi, A. Koochi, A.S. Kazemi, A. Yekrangi, M. Abadyan and M. Noghrehabadi, 2011. Analytical Approach to Compute the Internal Stress Field of NEMS Considering Casimir Forces. Procedia Engineering, 10: 3765-3771.
20. Adomian, G., 1988. A review of the decomposition method in applied mathematics. Journal of Mathematical Analysis and Applications, 135: 501-544.
21. Adomian, G., 1994. Solving Frontier Problems of Physics: The Decomposition Method. Kluwer Academic Publishers, Boston.
22. He, J.H., 1997. A new approach to nonlinear partial differential equations. Communications in Nonlinear Science and Numerical Simulation, 2 (4): 203-205.
23. He, J.H., 1999. Variational iteration method_A kind of nonlinear analytical technique: Some examples. International Journal of Non-Linear Mechanics, 34: 708-799.
24. He, J.H., 2000. A coupling method of a homotopy technique and a perturbation technique for non-linear problems. International Journal of Non-Linear Mechanics, 35: 37-43.
25. He, J.H., 2006. New interpretation of Homotopy perturbation method. International Journal of Modern Physics B, 20 (18): 2561-2568.
26. Adomian, G., 1983. Inversion of nonlinear stochastic operators. Journal of Mathematical Analysis and Applications, 91: 39-46.
27. Adomian, G., 1983. Stochastic Systems. Academic Press, London.
28. Rach, H., 1984. A convenient computational form for the Adomian polynomials. Journal of Mathematical Analysis and Applications, 102: 415-419.
29. Chiu, C.H. and C.K. Chen, 2002. A decomposition method for solving the convective longitudinal fins with variable thermal conductivity. International Journal of Heat and Mass Transfer, 45: 2067-2075.
30. Soroush, R., A. Koochi, H. Haddadpour, M. Abadyan and A. Noghrehabadi, 2010. Investigating the effect of Casimir and van der Waalsattractions on the electrostatic pull-in instability of nanoactuators. Physica Scripta, 82: 045801 (11pp).
31. Adomian, G., 1986. Nonlinear Stochastic Operator Equations. Academic Press, London.
32. Gabet, L., 1994. The theoretical foundation of the Adomian method. Computers & Mathematics with Applications, 27 (12): 41-52.
33. Wazwaz, A.M., 1999. A reliable modification of Adomian decomposition method. Applied Mathematics and Computation, 102: 77-86.
34. Koochi, A., A.S. Kazemi, Y. Tadi Beni, A. Yekrangid and M. Abadyan, 2010. Theoretical study of the effect of Casimir attraction on the pull-in behavior of beam-type NEMS using modified Adomian method. Physica E, 43 (2): 625-632.
35. Tadi Beni, Y., A. Koochi and M. Abadyan, 2011. Theoretical study of the effect of Casimir force, elastic boundary conditions and size dependency on the pull-in instability of beam-type NEMS. Physica E, 43 (4): 979-988.
36. Koochi, A., A.S. Kazemi and M. Abadyan, 2012. Influence of Surface Effect on Size-Dependent Instability of Nano-Actuator in Presence of Casimir Force. Physica Scripta, 85: 035804 (7pp).
37. Siddiqui, A.M., R. Mahmood and Q.K. Ghori, 2006. Homotopy perturbation method for thin film flow of a fourth grade fluid down a vertical cylinder. Physics Letters A, 352: 404-410.
38. Goodarzian, H., M. Ghobadi, M.A. Farahabadi, H. Mohammadnezhad and S.S. Hejazi, 2011. An investigation of nonlinear KdV type equations using HPM and VIM. Indian Journal of Science and Technology, 4 (8): 952-956.
39. Nayfeh, A.H., 1985. Problems in Perturbation. JohnWiley and Sons, New York.
40. He, J.H., 2006. Homotopy perturbation method for solving boundary value problems. Physics Letters A., 350: 87-88.
41. He, J.H., 2006. Some asymptotic methods for strongly nonlinear equations. International Journal of Modern Physics B., 20 (10): 1141-1199.
42. Ganji, D.D. and A. Sadighi, 2006. Application of He's Homotopy-perturbation Method to Nonlinear Coupled Systems of Reaction-diffusion Equations. International Journal of Nonlinear Sciences and Numerical Simulation, 7 (4): 411-418.